

---

EFDA–JET–CP(01)02-26

T.J.J. Tala, V.V. Parail, A. Becoulet, C.D. Challis, G. Corrigan, N.C.Hawkes,  
D.J. Heading, M.J. Mantsinen, S. Nowak  
and JET EFDA Contributors

# Impact of Different Preheating Methods on Q-Profile Evolution in JET



# Impact of Different Preheating Methods on Q-Profile Evolution in JET

T. J. J. Tala<sup>1</sup>, V.V. Parail<sup>2</sup>, A. Becoulet<sup>3</sup>, C.D. Challis<sup>2</sup>, G. Corrigan<sup>2</sup>,  
N.C.Hawkes<sup>2</sup>, D.J. Heading<sup>2</sup>, M.J. Mantsinen<sup>4</sup>, S. Nowak<sup>5</sup>  
and JET EFDA Contributors\*

<sup>1</sup>*Association Euratom-Tekes, VTT Chemical Technology, FIN-02044 VTT, Finland*

<sup>2</sup>*Euratom/UKAEA Fusion Association, Culham Science Centre, Abingdon, OX14 3DB, UK*

<sup>3</sup>*Association EuratomCEA, CEA-Cadarache, F-13108, St. Paul lez Durance, France*

<sup>4</sup>*Association EuratomTekes, Helsinki University of Technology, FIN-02015 TKK, Finland*

<sup>5</sup>*Association EuratomENEA-CNR, Istituto di Fisica del Plasma, 20133, Milano, Italy*

*\*See appendix of the paper by J.Pamela "Overview of recent JET results",*

*Proceedings of the IAEA conference on Fusion Energy, Sorrento 2000*

Preprint of Paper to be submitted for publication in Proceedings of the  
EPS Conference,  
(Maderia, Portugal 18-22 June 2001)

“This document is intended for publication in the open literature. It is made available on the understanding that it may not be further circulated and extracts or references may not be published prior to publication of the original when applicable, or without the consent of the Publications Officer, EFDA, Culham Science Centre, Abingdon, Oxon, OX14 3DB, UK.”

“Enquiries about Copyright and reproduction should be addressed to the Publications Officer, EFDA, Culham Science Centre, Abingdon, Oxon, OX14 3DB, UK.”

## ABSTRACT.

Recent results on JET indicate that high performance plasmas with only a moderate heating power can be reached with a reversed q-profile whereas with a monotonic q-profile, more power is needed to trigger the ITB and reach the same performance [1]. However, it is still not clear what the optimum target q-profile at the end of the preheating phase should be: deeply reversed, weakly reversed or monotonic. In order to assess and optimise how much off-axis current one can or should drive, which radial location to drive it, and where to deposit the external electron heating power so that the desired target q-profile could be achieved, detailed modelling of the q-profile evolution in the preheating phase has been done.

The current profile evolution during the preheating phase has been calculated with JETTO transport code [2] assuming neo-classical electrical conductivity. The following preheating methods are considered and compared: ohmic, LHCD, on-axis and off-axis minority hydrogen ICRH, on-axis and off-axis NBI as well as ECCD. The basic principle used in this study is that the power deposition and external current density profiles are calculated in a self-consistent way. Consequently, the codes to calculate the power deposition profiles are coupled to JETTO to allow a fully self-consistent simulation cycle between the transport and power deposition (plus current density) calculation with time. At present there are LHCD, NBI and ECRH/ECCD modules coupled to JETTO, but no ICRH module was found that would calculate the power deposition profiles roughly within the same time scale as the transport calculations are performed. Thus, ICRH power deposition profiles are calculated by a separate code.

## 1. EXPERIMENTAL RESULTS ON Q-PROFILE EVOLUTION ON JET

Different preheating methods can produce very distinct target q-profiles. The temporal evolution of the main plasma parameters for three different preheating scenarios in typical JET OS experiments is shown in Fig. 1. The main plasma parameters were the same for the three pulses, but what was distinct between the three pulses is the preheating method; one of them was with LHCD preheating (Pulse No: 51466), the second one with off-axis ICRF hydrogen minority preheating (Pulse No 51470) and the third one with ohmic preheating (Pulse No: 51456). The preheating phase lasted from  $t = 1.0\text{s}$  until  $t = 4.2\text{s}$  when NBI was switched on to make the MSE measurements. The target q-profiles just after the end of the preheating phase at  $t = 4.4\text{s}$  for these three different preheating methods are illustrated in Fig. 2. The q-profiles have been reconstructed with EFIT equilibrium code using the MSE measurements as the constraints for EFIT [3]. The q-profiles inside  $R = 3.6\text{m}$  are different between the three cases; LHCD and the off-axis ICRF preheating created a weakly reversed q-profile, but with a difference of 10cm in the radial location of  $q_{\text{min}}$  whereas ohmic preheating produced a monotonic q-profile. Also shown in Fig. 2 is the other LHCD preheated discharge with a higher magnetic field. This discharge yielded a deeply reversed q-profile inside  $R = 3.5\text{m}$ .

## 2. PREDICTIVE MODELLING OF DIFFERENT PREHEATING METHODS

The target  $q$ -profiles at  $t = 4.0$  s and  $t = 5.0$  s produced by the predictive modelling of the different preheating methods are compared in figure 3. In the simulations, the main plasma parameters and the initial and boundary conditions for  $T_e$  are taken from the Pulse No 51897. The external heating power is 5MW except in the case of LHCD when the power is 3MW. Thus, the simulations are identical except in terms of the heating and current drive methods. The preheating methods can be divided into three categories in terms of the created target  $q$ -profile. LHCD and ECCD form category 1 as being the only methods which can produce deeply reversed  $q$ -profiles. Quantitatively the  $q$ -profiles produced by LHCD and ECCD look quite similar. However, the central values of  $q$  are distinct. With LHCD,  $q$  tends to increase to very high values, such as  $q_0 \approx 30-50$  whereas in the case of ECCD,  $q_0$  remains between 10 and 20. This difference comes mainly from the amount of the driven off-axis current; LHCD driven current is of the order of 500900 kA whereas ECCD current is only 70160kA. Large off-axis current can transiently drive the the total current density in the core to zero, as has been recently observed in JET [3]. Category 2 consists of off-axis NBI and off-axis ICRH heating which create weakly reversed  $q$ -profiles with  $q_{\min}$  located inside  $R = 3.4$ m. On-axis NBI, on-axis ICRH and ohmic preheating belong to category 3 as they can only create monotonic target  $q$ -profiles. The power deposition profiles (electron channel) and the electron temperature profiles for the same preheating method scan, as shown in figure 3, are compared in figure 4.

## CONCLUSIONS

The driven current by LHCD, ECCD and off-axis NBI was found to be absolutely crucial to modify the  $q$ -profile evolution in the preheating phase. Without any external current driven by LHCD or ECCD, instead of having a deeply reversed target  $q$ -profile, a weakly or even a monotonic target  $q$ -profile was created. The timing scans indicated that the location of  $q_{\min}$  was insensitive to the start time of the preheating whereas the deepness of the shear reversal turned out to be very sensitive to it. The possible redistribution of the current by the sawtooth-like events arising presumably from neo-classical tearing modes or resistive interchange modes is not taken into account in the present modelling and may have an effect on the predictions.

## REFERENCES

- [1]. Challis C D et al. 2001 this conference.
- [2]. Genacchi G, and Taroni A 1988 JETTO: A free boundary plasma transport code (basic version), Rapporto ENEA RT/TIB 1988(5).
- [3]. Hawkes N C et al. 2001 this conference..

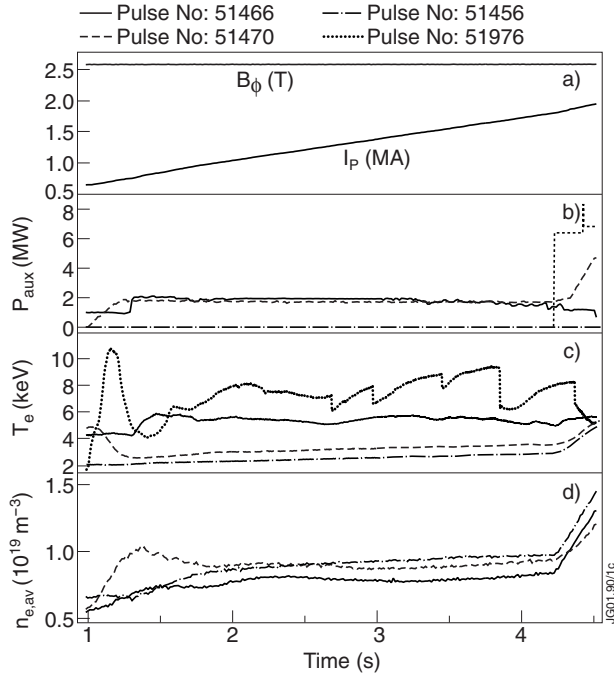


Figure 1: Time traces of plasma current and magnetic field (a), external heating powers (b), central electron temperatures (c) and average electron densities (d) for three discharges with different preheating methods. Solid curve refers to the pulse with LHCD preheating, dashed curve with ICRF preheating and dash-dotted curve with ohmic preheating. The NBI power (short dashed curve in (b)) started at  $t = 4.2\text{s}$  is the same for all the three discharges. The dotted curve in (c) is another LHCD preheated pulse with a higher  $B_\phi$

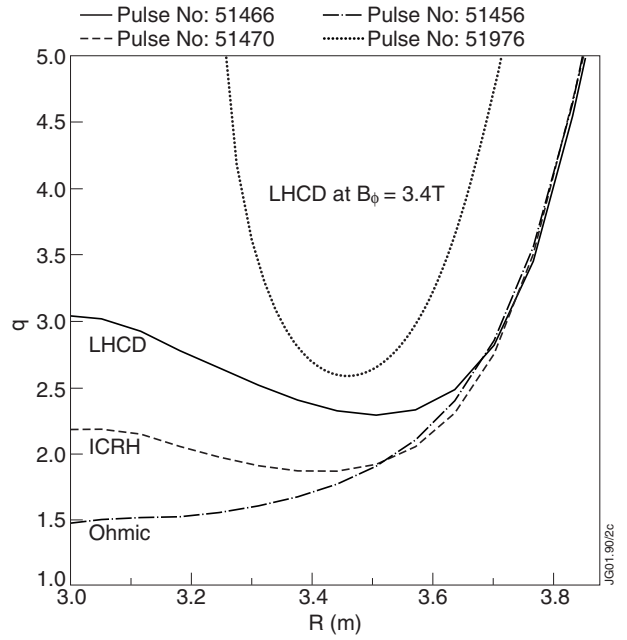


Figure 2:  $q$ -profiles at the end of the preheating phase for the different preheating schemes. Solid curve corresponds to LHCD preheating, dashed one to ICRF preheating and dash-dotted one to ohmic preheating. The dotted curve is the other LHCD preheated discharge at higher magnetic field and with a better plasma breakdown.

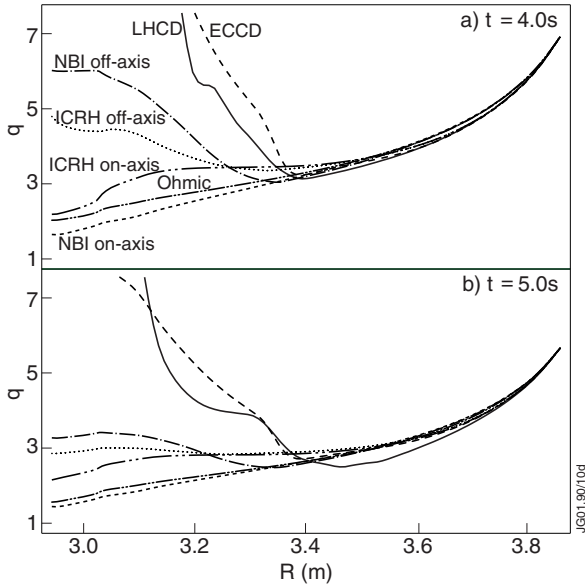


Figure 3: Target  $q$ -profiles produced with different preheating methods at  $t = 4.0\text{s}$  (a) and  $t = 5.0\text{s}$  (b). Category 1: LHCD (solid curve) and ECCD (dashed curve); category 2: off-axis NBI (dash-dotted curve) and off-axis ICRH (dotted curve); category 3: on-axis NBI (short dashed curve), on-axis ICRH (long double dot-dashed curve) and ohmic (short double dot-dashed curve).

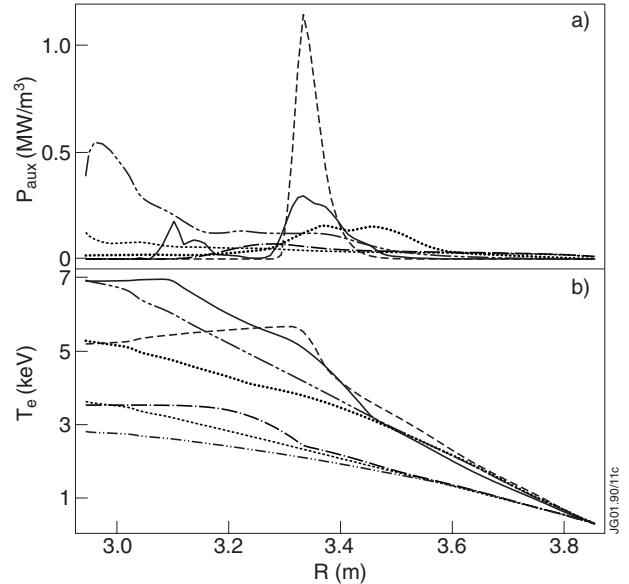


Figure 4: Power deposition profiles (electron channel) (a) and electron temperature profiles (b) at  $t = 5.0\text{s}$  for the same cases as shown in figure 3.